ChemPubSoc Europe

DOI: 10.1002/chem.201504268

CHEMISTRY A European Journal Full Paper

Host–Guest Systems

Metal-Cation Recognition in Water by a Tetrapyrazinoporphyrazine-Based Tweezer Receptor

Lukas Lochman,[a] Jan Svec,[a] Jaroslav Roh,[b] Kaplan Kirakci,[c] Kamil Lang,[c] Petr Zimcik,[a] and Veronika Novakova*[d]

Abstract: A series of zinc azaphthalocyanines with two azacrowns in a rigid tweezer arrangement were prepared and the fluorescence sensing properties were investigated. The size-driven recognition of alkali and alkaline earth metal cations was significantly enhanced by the close cooperation of the two azacrown units, in which both donor nitrogen atoms need to be involved in analyte binding to switch the sensor on. The mono- or biphasic character of the binding isotherms, together with the binding stoichiometry and magnitude of association constants (K_A), indicated specific complexation of particular analytes. Water solvation was shown to play an important role and resulted in a strong quenching of sensor fluorescence in the ON state. The lead compound was embedded into silica nanoparticles and advantageous sensing properties towards K^+ were demonstrated in water ($\lambda_F = 671$ nm, apparent $K_A = 82\ M^{-1}$, increase of 17×), even in the presence of (supra)physiological concentrations of Na^+ and Ca^{2+}.

Introduction

Cation binding by various synthetic receptors derived from crown ethers has been of interest in host–guest chemistry since the discovery of crown ethers by Pedersen in 1967.[1] Suitable supramolecular arrangements of crown ether analogues (such as cryptands,[2]coronands,[3] and lariat ethers[4]) may provide an incredible tool for selective cation recognition. Among them, the tweezer (occasionally also called sandwich or clamshell) arrangement of two crown units has been shown to substantially increase the stability of the complex (i.e., association constant) and improve selectivity towards specific analytes.[5,6] At the same time, a rigid arrangement was found to be the key factor for developing specific cation receptors in crown ether complexation.[6] Rigidity can be achieved, for example, by the introduction of an aromatic ring as one bond in the crown moiety (i.e., benzocrowns[6]). Clearly, the attachment of two crowns as close as possible may also lead to the formation of a rigid pocket that may improve the cooperation of the two crown moieties, similar to that observed in a simple molecule consisting of two crown moieties connected through a CH_2CH_2 bridge.[7] To the best of our knowledge, this possibility has not yet been investigated in fluorescence sensors and only compounds containing crown ethers separated from each other by four or more bonds have been reported.[8]

In general, the presence of a nitrogen atom in a crown moiety (forming so-called azacrowns) represents a useful tool for their binding to a signalling moiety simply through nucleophilic substitution. In addition, the lone pair on nitrogen forms a donor for photoinduced electron transfer (PET) or intramolecular charge transfer (ICT), which proceeds between the recognition and signalling moieties of a sensor.[9,10] These phenomena are responsible for the effective quenching of excited states; thus keeping the signalling moiety non-fluorescent (OFF state). Complexation of an analyte by an azacrown leads to a suppression of PET (or ICT), which results in switching of the signalling moiety to its fluorescent (ON) state.[9,11]

Undoubtedly, fluorescence analysis offers high sensitivity and an exceptionally low detection threshold, along with the possibility of time-resolved monitoring.[11] Consequently, fluorescent sensors are receiving attention for their potential application in areas such as biochemical and medical analysis (e.g., hypertension and bipolar disorder), cell biology (e.g., highlighting of cell compartments with high concentration of some cations) or in monitoring environment pollution by heavy metals.[11] For all of these applications, absorption and emission above $\lambda = 600$ nm are highly advantageous due to the limited interaction of the light with endogenous chromophores and substantially lower light scattering.[11]

[a] L. Lochman, Dr. J. Svec, Assoc. Prof. P. Zimcik
Department of Pharmaceutical Chemistry and Drug Control
Faculty of Pharmacy in Hradec Kralove, Charles University in Prague
Heyrovskeho 1203, 50005 Hradec Kralove (Czech Republic)
Homepage: http://portal.faf.cuni.cz/Groups/Azaphthalocyanine-group/

[b] Dr. J. Roh
Department of Inorganic and Organic Chemistry
Faculty of Pharmacy in Hradec Kralove, Charles University in Prague
Heyrovskeho 1203, 50005 Hradec Kralove (Czech Republic)

[c] Dr. K. Kirakci, Dr. K. Lang
Institute of Inorganic Chemistry, v.v.i., Czech Academy of Sciences
Husinec-Řež 1001, 250 68 Řež (Czech Republic)

[d] Assoc. Prof. V. Novakova
Department of Biophysics and Physical Chemistry
Faculty of Pharmacy in Hradec Kralove, Charles University in Prague
Heyrovskeho 1203, 50005, Hradec Kralove (Czech Republic)
E-mail: veronika.novakova@faf.cuni.cz

Supporting information and ORCID(s) from the author(s) for this article are available on the WWW under http://dx.doi.org/10.1002/chem.201504268.

This work is focused on developing a new type of rigid tweezer-like crown ether recognition moiety with two azacrowns attached in *ortho* positions to a tetrapyrazinoporphyrazine (TPyzPz) fluorophore (Figure 1). This close connection of

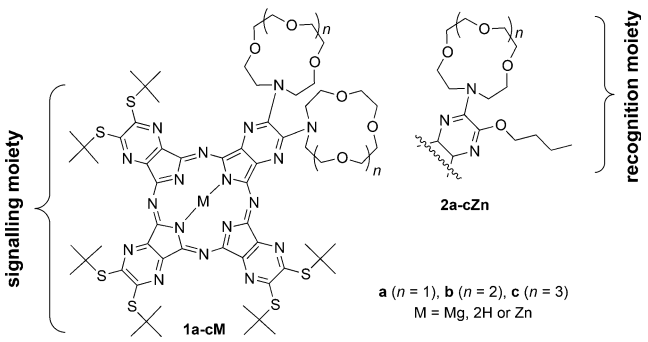

Figure 1. Structures of target sensors **1a–cM** with azacrown moieties in a tweezer-like arrangement. Compounds **2a–cZn**, described recently,[15] were used for comparison.

azacrowns may result in their improved cooperation, which is expected to substantially influence the selectivity toward different cations. TPyzPz, an aza analogue of phthalocyanine, is used herein as a signalling moiety. This fluorophore combines absorption and emission over $\lambda = 650$ nm with a high extinction coefficient (approximately 200 000 $mol^{-1} L cm^{-1}$) and advantageous fluorescence properties. Because of these ideal properties, TPyzPzs have recently been used to develop pH sensors for both acidic[12] and basic pH[13] and sensors for metal cations.[14,15] In the design of the TPyzPz macrocycle for the present project, the core was decorated with bulky *tert*-butylsulfanyl groups to hinder undesirable aggregation of the planar macrocyclic core. The zinc(II) cation in the TPyzPz centre (**1a–cZn**) ensures high stability and advantageous photophysical properties.[16]

The majority of fluorescence sensors that combine different fluorophores and crown ethers have been investigated in organic solvents (mostly acetonitrile); however, they may become ineffective in aqueous solutions because water solvation of metal cations limits cation binding.[17,18] From this perspective, it is also essential to examine the sensing properties of the novel tweezer arrangement in water.

Results and Discussion

Synthesis

In general, low-symmetry TPyzPzs are prepared through the mixed cyclotetramerisation of two different precursors A and B, that is, appropriate 5,6-disubstituted-pyrazine-2,3-dicarbonitriles. The desired precursors were synthesised through the nucleophilic substitution of 5,6-dichloropyrazine-2,3-dicarbonitrile with azacrowns of different cavity sizes, leading to **3a–c** in yields of 83, 55 and 82%, respectively (Scheme 1). Heating at reflux is necessary for complete conversion into the disubstituted product. Stirring the reaction at room temperature

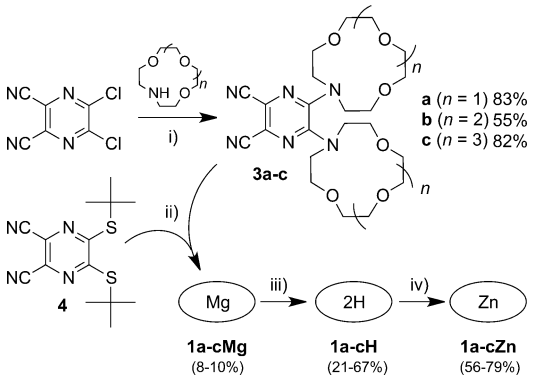

Scheme 1. Synthesis of precursors and target macrocycles: i) anhydrous K_2CO_3, THF, reflux; ii) $Mg(BuO)_2$, BuOH, reflux, chromatographic separation of target congener; iii) *p*-toluenesulfonic acid (TsOH), THF, RT; iv) $Zn(CH_3COO)_2$, pyridine, reflux.

always afforded a large portion of mono-substituted compound, even if a high excess of azacrown and/or prolonged reaction times of up to several days were applied. Precursor **4** with bulky *tert*-butylsulfanyl groups was synthesised by using a procedure similar to that previously reported by our group.[19]

Target TPyzPzs were prepared by the statistical condensation of precursors **3a–c** (A) and **4** (B) by using the Linstead method of cyclotetramerisation with magnesium butoxide as an initiator (Scheme 1). This reaction led to a statistical mixture of six magnesium congeners (AAAA, AAAB, AABB, ABBB, ABAB and BBBB), in which the probability of ABBB formation was increased by using a precursor ratio of 1:3 (A/B).[20] The required unsymmetrical congener of ABBB type was then isolated and purified by column chromatography. Although the separation of TPyzPz congeners is generally performed in the metal-free form due to their lower tendency towards tailing on silica,[21] the isolation of ABBB was performed as the magnesium complexes in this case. This was enabled by the completely different retention factors of TPyzPz congeners due to the significantly different properties of their peripheral substituents (lipophilic *tert*-butylsulfanyls versus highly hydrophilic azacrowns). Magnesium complexes **1a–cMg** were obtained in reasonable yields of 8–10% and were used as intermediates for further reaction steps. The magnesium cation was removed from the centre by TsOH, leading to metal-free derivatives **1a–cH**, which were then converted into target zinc complexes **1a–cZn** by treatment with zinc acetate in pyridine (Scheme 1).

Photophysical properties of the sensors in the OFF state

To characterise the properties of the sensors in their OFF state, their spectral and fluorescence properties were investigated in THF. All of the prepared TPyzPzs exhibited absorption spectra typical for phthalocyanines and their analogues with a high-energy B band at $\lambda = 380$ nm and a low-energy Q band at $\lambda \approx 655$ nm (Figure 2d). Interestingly, the Q band of the metal complexes appeared as a single narrow band, which was atypical for low-symmetry phthalocyanines.[22] This feature can be

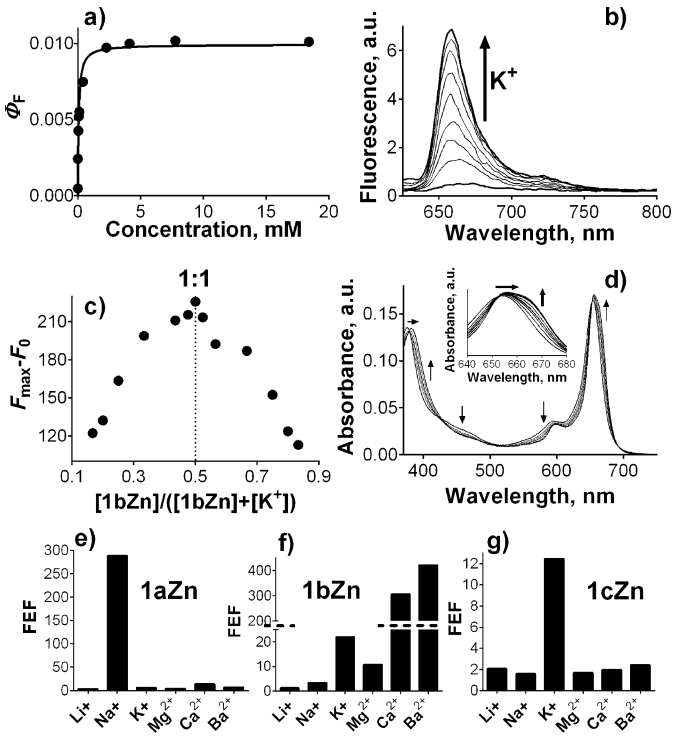

Figure 2. Sensing properties in THF. a) Dependence of Φ_F of **1 bZn** on the concentration of added K^+. b) Fluorescence emission spectra of **1 bZn** (1 μM) during titration with K^+. c) A Job plot for the interaction of **1 bZn** with K^+ ($c_{(K^+ + 1\,bZn)} = 10$ μM). d) Absorption spectra of **1 bZn** (1 μM) during titration with K^+. Fluorescence enhancement factors (FEFs) of **1 aZn** (e), **1 bZn** (f) and **1 cZn** (g) with different cations at complete binding.

explained by the fact that both alkylsulfanyl and alkylamino substituents contribute to the system of π-conjugated bonds in a similar way.[14,15] In contrast, the metal-free derivatives **1 a–cH** possessed a typical split Q band due to a pronounced loss of symmetry caused by central hydrogen atoms.

After excitation, compounds **1 a–cZn** emitted barely detectable red fluorescence at $\lambda \approx 660$ nm characterised by fluorescence quantum yields (Φ_F) of less than 0.001. Such low Φ_F values are caused by ultrafast ICT between donor amines of the azacrown moieties to the TPyzPz core (i.e., acceptor).[21] These results are in good agreement with our previous study on the structural aspects that influence ICT.[21,23] Specifically, the presence of two nitrogen donors on the TPyzPz core guarantees nearly complete quenching of the excited states, and therefore, the OFF state of the sensors is almost non-fluorescent.

Sensing properties in THF

The sensing properties of TPyzPzs **1 a–cZn** towards cations were assessed in THF. In the case of sensitive analytes, stepwise titration with alkali and alkaline earth metal perchlorates in MeOH led to changes in both the absorption and fluorescence emission spectra. Consistent with our previous data,[15] the absorption Q band shifted negligibly (Figure 2 d). These slight changes in absorption spectra are caused by a different contribution of peripheral nitrogen atoms to the system of π-conjugated bonds of TPyzPz, and may also be considered as proof of an analyte–sensor interaction. Changes in fluorescence intensity were considerably more pronounced (Figure 2 b). The increase in fluorescence intensity is attributed to the suppression of the ICT process and restoration of emissive relaxation pathways. The FEF, which represents the increase in fluorescence intensity from the OFF to ON state, reached high values of greater than 100 in several cases (Table 1 and Figure 2 e–g). A comparison of FEFs for different cation–sensor combinations (Figure 2 e–g) revealed preferential binding of cations. Briefly, compound **1 aZn** was sensitive to Na^+ only; compound **1 bZn** recognised K^+, Ca^{2+} and Ba^{2+} with different association constants (see below); and **1 cZn** was specific towards K^+. In some titration curves (e.g., Figures S1 c and S3 b–e in the Supporting Information), fluorescence intensity decreased as more cation was added after the plateau phase was reached. This may be caused by negligible sensor aggregation due to the high ionic strength of the solution. At the same time, an enhancement of the thermodynamic feasibility of ICT due to increasing polarity of the medium with increasing volume of MeOH may lead to greater quenching of the excited states.[24] This phenomenon occurred at higher concentrations of analytes and did not significantly influence the relationships discussed below.

Table 1. Spectral and photophysical properties of **1 a–cZn** in the OFF state and after complete binding in THF.[a]

	Φ_F[b] (λ_F [nm])	Bind.[c]	K_A [M^{-1}] (FEF_1)[d]	Total FEF[e]
1 aZn	0.00023 (656)			
+ Mg^{2+}	0.00090 (658)	bi	15 000 (1.4)	3.9
+ Li^+	0.00064 (657)	bi	–[f]	2.8
+ Ca^{2+}	0.0031 (660)	bi	60 000 (1.3)	14
+ Na^+	0.067 (657)	bi	21 000 (7.7)	291
+ Ba^{2+}	0.0016 (659)	bi	189 000 (1.8)	6.9
+ K^+	0.0013 (660)	mono	28 000 (5.7)	5.7
1 bZn	0.00046 (656)			
+ Mg^{2+}	0.0050 (656)	bi	129 000 (1.4)	11
+ Li^+	0.00059 (656)	bi	110 (1.3)	1.3[g]
+ Ca^{2+}	0.14 (657)	bi	25 (78.8)	304
+ Na^+	0.0016 (657)	bi	20 000 (1.6)	3.5
+ Ba^{2+}	0.19 (657)	mono	15 (413)	413
+ K^+	0.010 (658)	mono	14 000 (22)	22
1 cZn	0.0010 (658)			–
+ Mg^{2+}	0.0011 (661)	–[f]	–[f] (1.7)	1.7[g]
+ Li^+	0.00072 (659)	–[f]	–[f] (2.1)	2.1[g]
+ Ca^{2+}	0.0020 (659)	–[f]	–[f] (2.0)	2.0[g]
+ Na^+	0.0017 (662)	–[f]	–[f] (1.7)	1.7[g]
+ Ba^{2+}	0.0025 (659)	–[f]	18 000 (2.5)	2.5[g]
+ K^+	0.013 (661)	–[f]	720 000 (13)	13[g]

[a] Fluorescence emission maximum (λ_F), fluorescence quantum yield (Φ_F), fluorescence enhancement factor (FEF), association constant (K_A), proposed character of binding (Bind.). [b] Unsubstituted zinc phthalocyanine was used as a reference ($\Phi_F = 0.32$ in THF). [c] Mono- (mono) or biphasic (bi). [d] K_A and FEF for the first step of the titration curve; total concentration of the sensors $c = 1$ μM; K_A was determined from Φ_F (see the Supporting Information). [e] FEF for complete binding (i.e., calculated from Φ_F corresponding to the binding of two cations in the case of biphasic character). [f] Not possible to determine. [g] FEF for the first increase in fluorescence, even if biphasic character was anticipated.

From the perspective of the azacrown size, the tweezer crown arrangement substantially affected the selectivity of recognition in comparison with the corresponding monocrown sensors **2a–cZn** reported recently.[15] It was shown that **2aZn**, with 1-aza[12]crown-4, preferentially bound small ions, such as Li^+ and Na^+; **2bZn**, with 1-aza[15]crown-5, bound both Na^+ and K^+; and **2cZn**, with 1-aza[18]crown-6, predominantly bound K^+. However, the reported selectivities were rather modest; in addition, the binding of alkaline earth metal cations (Ca^{2+}, Ba^{2+} and Mg^{2+}) was strong and independent of the size of the divalent cations.[15] Clearly, this problem was overcome in the **1a–cZn** series, in which the rigidity of the recognition system limited the number of cations that fit well into the recognition moiety. In general, the crown tweezer recognised larger cations better than the monocrown series (e.g., 1-aza[12]crown-4 of **1aZn** binds Na^+ rather than Li^+ bound by the corresponding **2aZn**, 1-aza[15]crown-5 of **1bZn** binds K^+ only rather than both Na^+ and K^+ recognised by the corresponding **2bZn**). In addition to the selectivity, the tweezer arrangement also significantly improved the sensitivity of the sensors because the interactions proceeded with high association constants (K_A; i.e., low concentration of analytes). For example, the K_A of the K^+/1-aza[15]crown-5 interaction increased from 970 M^{-1} of **2bZn**[14] to 14000 M^{-1} of the corresponding **1bZn**. This high value is advantageous due to switching of the sensor to the ON state at a very low concentration of the analyte.

By examining the course of the titration experiments in more detail, it is clear that the binding process for **1a–cZn** is completely different from that of **2a–cZn**, in which the titration curves of all cations follow a one-site binding isotherm. In the case of **1a–cZn**, biphasic titration curves were frequently observed in addition to the monophasic ones. Theoretically, two cations can be coordinated in both azacrowns simultaneously (i.e., sensor/cation stoichiometry of 1:2; Figure 3b) or one cation is coordinated by two azacrowns (stoichiometry of 1:1; Figure 3a). In the former case, two cations need to be coordinated in both azacrowns simultaneously for switching the sensor to the ON state because one remaining free donor still effectively quenches the excited states of the sensor through ICT. Such outstanding quenching is typical for alkylamino TPyzPzs and is not usually so effective in other groups of acceptor moieties.[25]

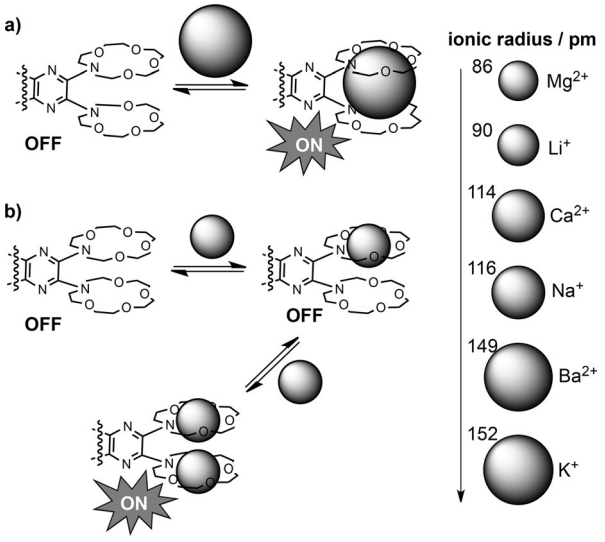

Figure 3. Proposed model of cation binding into tweezer TPyzPz discriminated by the ionic radius of the metal cation and subsequent switching to the ON state. a) 1:1 stoichiometry. b) 1:2 stoichiometry.

A biphasic character was observed for the titration curves with the cations fitting well or being smaller than the cavity of the corresponding azacrowns (Figure 4, Table 1, and Figures S1–S3 in the Supporting Information). The K_A values of the first step were generally quite high, but were accompanied by only a negligible increase in fluorescence, typically in the range of 1.3- to 1.8-fold. In accordance with the proposed mechanism of stepwise binding (Figure 3b), the second step of the titration curve was observed at higher analyte concentrations (typically 200–400 mM), which suggested K_A values of less than 10 M^{-1}. However, it was not possible to determine exact K_A values of the second titration step because of the complex character of binding, which involved steric factors when two cations would not easily fit close together. The biphasic character was also anticipated for some combinations in which only monophasic character was observed (e.g., **1cZn**/K^+ and **1cZn**/Ba^{2+}); but the binding of the second cation was apparently too weak to be detected in the cation concentrations tested (up to 400 mM). Thus, only monophasic character with a rather low FEF was observed, which indicated that only one crown unit was occupied.

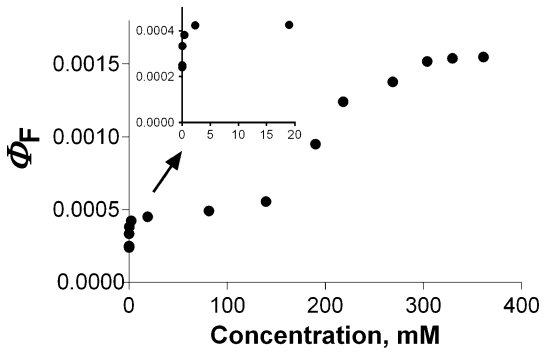

Figure 4. An example of a biphasic response to an analyte (dependence of Φ_F of **1bZn** on the concentration of the added Na^+) in THF.

In contrast, monophasic titration curves with a rapid increase in fluorescence with FEF values ranging from 22 to 413 were observed for metal cations that were larger than the appropriate crown cavity (e.g.,**1bZn**/K^+ and **1bZn**/Ba^{2+}). This behaviour suggests the organisation of cations into the tweezer with efficient blocking of the ICT on both donor crown nitrogen atoms (Table 1 and Figure 3a). The binding stoichiometry assessed by the Job method of continuous variation (Figure 2c) was found to be 1:1, which further supported this premise.

Clearly, the combination of size-driven complexations and rigidity of the tweezer recognition moiety significantly affects both selectivity and sensitivity towards specific cations. Consequently, sensors that are selective and sensitive at low concentrations of an analyte may be prepared by using the described tweezer recognition moiety. For example, compound **1 bZn** with a good K_A value for K^+ ($K_A = 14000\ M^{-1}$) is highly advantageous due to switching to the ON state at a low concentration of this analyte and possessing very well distinguished selectivity between Na^+ and K^+. Even if this compound is also sensitive to Ca^{2+} and Ba^{2+}, more than 10^3 times higher concentrations of these cations, relative to K^+, are necessary to switch the sensor on, which, naturally, cannot be considered as biologically relevant. To demonstrate the selectivity of **1 bZn** to K^+, titration experiments in THF in the presence of a physiological level of Na^+ (5 mM in resting cells)[11] were performed (Figure S7 in the Supporting Information). Clearly, the course of the titration curve was not significantly affected. However, an increased amount of salts in the organic solvent led to the formation of a microsuspension that prevented experiments from being performed at higher concentrations of Na^+ (physiological concentration of Na^+ in plasma is 135–148 mM) or with other competitive cations. Thus, detailed competitive experiments were performed in water with the sensor embedded into nanoparticles (**1 bZn@NP**), for which the solubility of the cations and sensor was not the limiting factor (see below).

The fact that the character of binding is not straightforward, but may be a consequence of the combined effects of more factors, can be demonstrated by biphasic Na^+ binding into **1 aZn**. The relatively high K_A ($21000\ M^{-1}$) with a modest FEF_1 (7.7) for the first step in the titration curve indicates that Na^+ is large enough to bind efficiently first as a tweezer (Figure 3 a). As the concentration of Na^+ in the solution increases, two-cation binding (Figure 3 b) becomes preferable. This results in a further increase in fluorescence, reaching a total FEF of 291.

Effect of water on cation–sensor interactions

In addition to size-driven complexation, there are other factors involved in the host–guest chemistry of crown ethers, for example, the replacement of oxygen for different heteroatoms, crown isomerisation/spatial organisation and solvation effects. The last of these is accepted to be one of the most important.[26] The size of the cation may increase due to solvation and, as a consequence, size suitability for a particular crown ether may partially change. Furthermore, different crown conformations[17] may form with respect to the solvating molecules. Thus, solvation may substantially affect binding in the crown ethers. These effects can be deduced from the Gutmann donor number,[27] in which a higher value indicates stronger solvation. Water (Gutmann donor number of 18), MeOH (19) and THF (20) strongly solvate cations, whereas common organic solvents, such as acetonitrile (14.1), benzonitrile (11.9) and dichloromethane (1.0), do not have this pronounced ability.[28] Water was reported by Rounaghi and Mofazzeli to play a very important role in cation–crown interactions; this showed that the stability of the complexes increased as the concentration of water was lowered in binary mixtures of MeOH/water.[29]

To investigate the role of water in the sensing properties of the studied TPyzPzs, fluorescence titration experiments were performed in anhydrous solvents. The addition of K^+ in anhydrous MeOH into a solution of **1 bZn** in anhydrous THF resulted in FEF values that were almost two-fold larger (Figure 5 a)

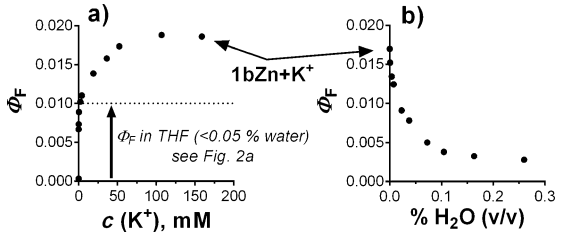

Figure 5. The effect of water on the fluorescence quantum yield of **1 bZn**/K^+. a) Stepwise addition of KSCN (in anhydrous MeOH) to a solution of **1 bZn** in anhydrous THF. The horizontal line represents a Φ_F value achieved in THF (HPLC grade, water content of $<0.05\%$. b) Stepwise addition of water to a solution of **1 bZn** in anhydrous THF containing KSCN (in anhydrous MeOH).

than those obtained in the experiment mentioned above in commercially available THF with a water content of $<0.05\%$. By studying the role of water in more detail on a model compound, **1 bZn**, in the presence of sensitive cations (K^+, Ba^{2+} and Ca^{2+}), we discovered that only traces of water led to a steep decrease in fluorescence quantum yields (Figure 5 b and Figure S4 in the Supporting Information).

It is therefore evident that, despite the high solvation ability of THF, based on the Guttmann donor number, which is comparable to that of water, the results in this solvent do not have to simulate real behaviour in water. Thus, the sensing properties of **1 bZn** were studied in water after the sensor was embedded into silica nanoparticles (see below).

Sensing properties in water

Based on the relationships disclosed above, compound **1 bZn** was chosen as a model compound because it was sensitive to K^+ with good K_A and FEF values. It is also sensitive to higher levels of other cations at (Ba^{2+} and Ca^{2+}) and experiments may determine whether the results obtained in THF can be extrapolated to water. Silica nanoparticles of **1 bZn@NP** were prepared by hydrolysis and condensation of triethoxyvinylsilane silicate precursor in a water-in-oil microemulsion containing **1 bZn**. The nanoparticles exhibited an average hydrodynamic diameter of approximately 13 nm, as measured by dynamic light scattering, which was in accordance with TEM observations (Figures S9 and S10 in the Supporting Information). These nanoparticles have been previously found to be suitable nanocarriers for monoazacrown TPyzPz sensors in aqueous solutions.[14] The absorption spectra of a dispersion of the nanoparticles (Figure S6 in the Supporting Information) revealed that the monomeric character of the sensor was preserved. This feature is essential for proper functioning of the sensor.

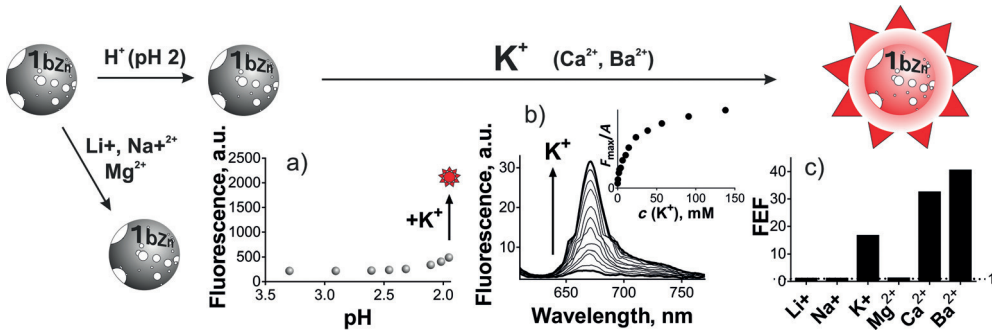

Figure 6. Sensing of **1 bZn@NP** in water. a) The sensor remains in the OFF (non-fluorescent) state upon titration with AcOH (from neutral down to pH 2) and switches on only after the addition of K^+. b) Changes in fluorescence emission spectra during titration of K^+ in water (pH 2). Inset: Titration of **1 bZn@NP** in water (pH 2) with K^+. Fluorescence intensity was corrected for changes of absorbance at the excitation wavelength. c) FEFs of **1 bZn@NP** with different cations at complete binding.

Compound **1 bZn@NP** was first studied under acidic conditions because fluorescent sensors based on the ICT mechanism generally suffered from false positive results caused by protonation of tertiary amines typically used as electron donors. Protonation of a donor amine may block the ICT even more strongly than cation coordination and may lead to misinterpretation of the results. Stepwise acidification down to pH 2 did not affect the fluorescence of **1 bZn@NP** (Figure 6). It is caused by the direct connection of donor nitrogen atoms to the TPyzPz core, which makes them almost non-basic ($pK_A = -2.5$; estimated by calculation using Advanced Chemistry Development Software V8.14). Therefore, compound **1 bZn@NP** can be considered to be insensitive to the pH of the medium.

Interestingly, almost identical dependences to those found in THF were observed upon the titration of **1 bZn@NP** with different alkali and alkaline earth metal cations in water (Figure 6, Table 2, and Figure S5 in the Supporting Information). Thus, the stepwise addition of K^+ led to a steep increase in fluorescence with a FEF of 17 ($K_A = 82\ M^{-1}$). Analytes such as Na^+, Mg^{2+} and Li^+ had no effect on the fluorescence intensity. In the case of Ca^{2+} and Ba^{2+}, an increase in fluorescence intensities required several orders of magnitude higher concentrations than that of K^+. Such high concentrations of Ca^{2+} and Ba^{2+} are expected to be irrelevant for biological applications and make **1 bZn@NP** selective to K^+ only. This statement was further proved by the titration of **1 bZn@NP** with K^+ in the presence of biologically relevant analytes, namely, Na^+ and Ca^{2+}, at their physiological and supraphysiological concentrations (Figure 7 and Figure S8 in the Supporting Information).

Table 2. Spectral and photophysical properties of **1 bZn@NP** in water.[a]

	λ_F [nm]	K_A [M^{-1}]	Total FEF[b]
1 bZn@NP	669		
1 bZn@NP + K^+	671	82	17
1 bZn@NP + Ca^{2+}	668	–[c]	32
1 bZn@NP + Ba^{2+}	668	–[c]	40

[a] Fluorescence emission maximum (λ_F), apparent association constant (K_A), and fluorescence enhancement factor (FEF). [b] Calculated as F_{max}/F_0, in which F_{max} is the fluorescence intensity at complete binding and F_0 is the fluorescence intensity of the sensor without analyte. [c] Not possible to determine.

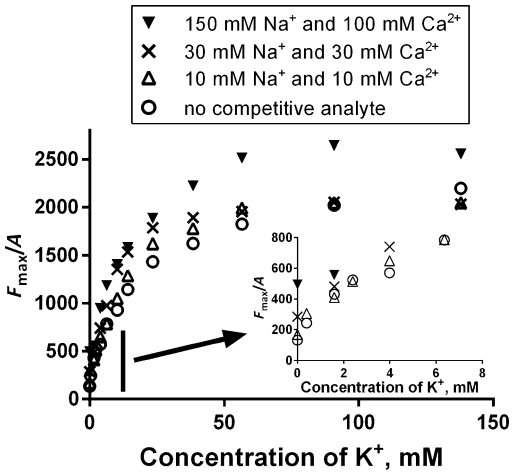

Figure 7. Titration of **1 bZn@NP** in water/acetic acid (3:1; $c_{(TPyzPz)} = 1\ \mu M$) with K^+ in the presence of different concentrations of Na^+ and Ca^{2+}.

Typical concentrations of Na^+ and Ca^{2+} in plasma are 135–148 and 2.1–2.8 mM, respectively, and in resting cells are 5 and 50–200 nM, respectively.[11] Interestingly, the presence of competitive analytes had no effect on the course of the titration curves; typically a slight increase in fluorescence intensity for the OFF state of the sensor was observed (Figure 7, inset). Even at supraphysiological levels of Na^+ (150 mM) and Ca^{2+} (100 mM), compound **1 bZn@NP** retained satisfactory sensing properties for K^+ with a FEF value of >5.

Potassium-binding benzofuranisophthalate (PBFI) and CD 222, which are two of the most widely used water-soluble fluorescence sensors for K^+, possess FEF values of 3.0 ($K_A = 200\ M^{-1}$) and 3.7 ($K_A = 1110\ M^{-1}$) in water, respectively.[11] Moreover, these sensors absorb at lower wavelengths ($\lambda = 336$ and 396 nm, respectively) with emission at $\lambda = 557$ and 480 nm, respectively. From this point of view, the FEF of 17 for **1 bZn@NP**/K^+ together with red emission at $\lambda = 671$ nm appear to be highly interesting.

Finally, these results confirm that the prepared sensors may also operate in water, which is always challenging in the field of synthetic fluorescence sensors, and that the dependences disclosed in the first part of the project may also be applied to the real behaviour of **1a–cZn** in water.

Conclusion

A series of zinc TPyzPz sensors, **1a–cZn**, with two azacrowns attached close to each other (in *ortho* positions on the pyrazine ring) were prepared. The compounds of the series differed in terms of the size of azacrowns used. This novel tweezer-like arrangement brought the possibility of close cooperation of crown moieties on the basis of increased rigidity of the entire recognition system. This was clearly demonstrated by comparison with a series of monoazacrown TPyzPz sensors: **2a–cZn**. The rigid tweezer-like arrangement of **1a–cZn** was responsible for the specific selectivity and sensitivity towards the analytes. Of greatest importance, the sensing of K^+ by **1bZn**, with a good K_A value of 14000 M^{-1} and good FEF of 22 in THF, is useful for the sensing of low K^+ levels and for thoroughly distinguishing between Na^+ and K^+, which are the analytes that generally occur together.

Furthermore, solvation, and particularly water solvation, was shown to play an important role in sensor–cation interactions. The fluorescence intensity upon titration with sensitive analytes was even more pronounced under anhydrous conditions because the crown recognition moiety did not need to compete with water for the cations.

Therefore, the sensing properties were further studied in water. For this purpose, compound **1bZn**, as a model compound, was embedded into silica nanoparticles (**1bZn@NP**). Interestingly, similar relationships to those observed in THF were observed in water. Compound **1bZn@NP** was switched on at a low concentration of K^+ (with FEF = 17, K_A = 82 M^{-1}), but required considerably higher levels of Ca^{2+} and Ba^{2+} to become fluorescent. Competitive titration experiments to study the sensitivity towards K^+ in the presence of biologically relevant cations (Na^+, Ca^{2+}) demonstrated that the rigid tweezer-like arrangement of azacrown recognition moiety could be a useful tool for the selective and sensitive recognition of cations in water.

Experimental Section

General

All of the organic solvents were of analytical grade. Anhydrous butanol was stored over magnesium and distilled prior to use. All chemicals for syntheses were obtained from established suppliers (Sigma-Aldrich, Acros, Merck, and TCI Europe) and used as received. THF used for the photophysical experiments of **1a–cZn** was of HPLC quality, with a water content of < 0.05% (purchased from Sigma-Aldrich). Anhydrous THF and MeOH were obtained through the distillation of THF (HPLC, water content of < 0.05%, Sigma Aldrich) or MeOH (HPLC, water content < 0.03%, Sigma-Aldrich) over sodium under an argon atmosphere. TLC was performed on Merck aluminium sheets with silica gel 60 F254. Merck Kieselgel 60 (0.040–0.063 mm) was used for column chromatography. Melting points were measured on an Electrothermal IA9200 Series digital melting point apparatus (Electrothermal Engineering Ltd., Southend-on-Sea, Essex, UK).^{1}H and ^{13}C NMR spectra were recorded on Varian Mercury Vx BB 300 or VNMR S500 NMR spectrometers. The reported chemical shifts are given relative to $Si(CH_3)_4$, and were locked to the signal of the solvent. IR spectra were measured on a Nicolet 6700 (ATR mode) spectrometer. The UV/Vis spectra were recorded by using a Shimadzu UV-2600 spectrophotometer. The fluorescence spectra were obtained by using an AMINCO Bowman Series 2 luminescence spectrometer. Elemental analysis was carried out on an Automatic Microanalyser EA1110CE (Fisons Instruments S.p.A., Milano, Italy) instrument. HRMS spectra were measured by using the UHPLC system Acquity UPLC I-class (Waters, Milford, USA) coupled to a high-resolution mass spectrometer Synapt G2Si (Waters, Manchester, UK) based on Q-TOF. Chromatography for the HRMS measurements was performed by using an Acquity UPLC BEH300 C4 (2.1 × 50 mm, 1.7 μm) column with isocratic elution with acetonitrile and 10 mM ammonium formate buffer pH 3 (90:10) at a flow rate of 0.4 mL min^{-1}. Electrospray ionisation (ESI) was operated in positive mode. The ESI spectra were recorded in the range of *m/z* 200–2000 by using glu-fibrinopeptide B as a lock mass reference and sodium iodide for calibration. MALDI-TOF mass spectra were recorded in the positive reflectron mode on a 4800 MALDI-TOF/TOF mass spectrometer (AB Sciex, Framingham, MA, USA) by using *trans*-2-[3-(4-*tert*-butylphenyl)-2-methyl-2-propenylidene]malononitrile as the matrix. The instrument was calibrated externally with a five-point calibration by using Peptide Calibration Mix 1 (LaserBio Labs, Sophia- Antipolis, France). 5,6-Dichloropyrazine-2,3-dicarbonitrile was purchased from TCI Europe. Precursor **4** was prepared according to a published procedure.[19]

General procedure for the synthesis of precursors 3a–c

The appropriate azacrown was added to a suspension of finely ground anhydrous K_2CO_3 in THF. 5,6-Dichloropyrazine-2,3-dicarbonitrile was then slowly added. The mixture was heated under reflux for 3–4 h. THF was evaporated, chloroform and one drop of hydrochloric acid were added, and the product was washed three times with brine. The organic layer was collected, filtered, and evaporated to dryness. The crude product was purified by column chromatography on silica gel (mobile phases are mentioned at each compound below). The product was thoroughly dried under reduced pressure.

5,6-Di(1,4,7-trioxa-10-azacyclododecan-10-yl)pyrazine-2,3-dicarbonitrile (3a): 5,6-Dichloropyrazine-2,3-dicarbonitrile (318 mg, 1.60 mmol), 1-aza[12]crown-4 (1.0 g, 5.74 mmol), anhydrous K_2CO_3 (1.1 g, 7.97 mmol), reaction time 3 h, eluent: chloroform/acetone 5:1 (R_f = 0.20), product was washed with hexane. Yield: 631 mg (83%) of light yellow solid; m.p. 137.4–138.0 °C; ^{1}H NMR (500 MHz, [D$_6$]acetone, 25 °C): δ = 3.54–3.59 (m, 16H; crown-H), 3.73–3.81 ppm (m, 16H; crown-H); ^{13}C NMR (125 MHz, [D$_6$]acetone, 25 °C): δ = 49.9, 70.1, 70.6, 71.9, 116.0, 119.8, 147.4 ppm; IR (ATR): $\tilde{\nu}$ = 2961, 2908, 2869, 2229 (CN), 2176, 1931, 1701, 1654, 1518, 1485, 1448, 1420, 1389, 1378, 1359, 1344, 1297, 1273, 1255, 1240, 1219, 1155, 1131, 1116, 1107, 1096, 1058, 1039, 1007, 970 cm^{-1}; elemental analysis calcd (%) for $C_{22}H_{32}N_6O_6$: C 55.45, H 6.77, N 17.64; found: C 55.32, H 6.80, N 17.50.

5,6-Di(1,4,7,10-tetraoxa-13-azacyclopentadecan-13-yl)pyrazine-2,3-dicarbonitrile (3b): 5,6-Dichloropyrazine-2,3-dicarbonitrile (500 mg, 2.51 mmol), 1-aza[15]crown-5 (1.16 g, 5.29 mmol), anhydrous K_2CO_3 (1.73 g, 12.56 mmol), reaction time 4 h, eluent: chloro-

form/acetone 5:1 (R_f = 0.09), product was washed with hexane. Yield: 785 mg (55%) of light yellow solid; m.p. 107.7–108.6 °C; ^{1}H NMR (500 MHz, $CDCl_3$, 25 °C): δ = 3.58 (s, 16H; crown-H), 3.63 (s, 8H; crown-H), 3.64–3.71 ppm (m, 16H; crown-H); ^{13}C NMR (125 MHz, $CDCl_3$, 25 °C): δ = 50.0, 69.1, 70.1, 70.3, 71.1, 115.0, 119.8, 146.5 ppm; IR (ATR): $\tilde{\nu}$ = 2871, 2225 (CN), 1735, 1538, 1517, 1492, 1438, 1410, 1347, 1291, 1267, 1245, 1218, 1179, 1115, 1097, 1081, 1065, 1040, 1017, 990 cm^{-1}; elemental analysis calcd (%) for $C_{26}H_{40}N_6O_8$: C 55.31, H 7.14, N 14.88; found: C 55.65, H 7.61, N 14.95.

5,6-Di(1,4,7,10,13-pentaoxa-16-azacyclooctadecan-16-yl)pyrazine-2,3-dicarbonitrile (3c): 5,6-Dichloropyrazine-2,3-dicarbonitrile (410 mg, 2.06 mmol), 1-aza[18]crown-6 (1.63 g, 6.19 mmol), anhydrous K_2CO_3 (1.42 g, 10.31 mmol), reaction time 3 h, eluent: chloroform/MeOH 15:1 (R_f = 0.25). Yield: 1.10 g (82%) of light yellow oil; ^{1}H NMR (500 MHz, [D$_6$]acetone, 25 °C): δ = 3.51 (s, 16H; crown-H), 3.56–3.63 (m, 16H; crown-H), 3.67 (t, J = 5 Hz, 8H; crown-H), 3.83 ppm (t, J = 5 Hz, 8H; crown-H); ^{13}C NMR (125 MHz, [D$_6$]acetone, 25 °C): δ = 49.6, 69.5, 70.8, 71.3, 71.4, 71.9, 116.2, 120.0, 147.9 ppm; IR (ATR): $\tilde{\nu}$ = 2864, 2224 (CN), 1948, 1529, 1517, 1486, 1437, 1350, 1293, 1249, 1220, 1119, 946 cm^{-1}.

General procedure for the synthesis of 1a–cMg

Magnesium turnings (28 equiv) and a small crystal of iodine were suspended in freshly distilled anhydrous *n*-butanol. The suspension was heated under reflux for 3 h until magnesium butoxide was formed. An appropriate compound, **3a**, **3b** or **3c** (precursor A; 1 equiv), was dissolved in freshly distilled anhydrous *n*-butanol and added in one portion to the reaction mixture. Then, compound **4** (precursor B; 3 equiv) was quickly added to the mixture all at once. The mixture was heated under reflux for 5 h. The solution was cooled and *n*-butanol was partially evaporated under reduced pressure. A mixture of water/MeOH/acetic acid 10:3:1 (v/v) was poured into the product and stirred for 1 h at RT. The dark green solid was collected by filtration, subsequently washed several times with water, and dried. The unsymmetrical congener (ABBB type) was isolated and purified by column chromatography on silica gel. The mobile phases and number of repetitions are mentioned for each compound below. The product was scratched into hexane, and then thoroughly dried under reduced pressure. The magnesium complexes were characterised by MS and used as intermediates for the next reaction.

Compound 1aMg: Mg (895 mg, 36.82 mmol), **3a** (626 mg, 1.31 mmol), **4** (1.21 g, 3.94 mmol), eluent: chloroform/THF 5:1 (R_f = 0.22) (purified twice). Yield: 153 mg (8%) of green solid; MS (MALDI-TOF): *m/z*: 1418.4 $[M]^+$, 1441.4 $[M+Na]^+$; HRMS (ESI$^+$): *m/z* calcd for $C_{64}H_{86}MgN_{18}O_6S_6$ $[M+H]^+$: 1419.5231; found: 1419.5210.

Compound 1bMg: Mg (880 mg, 36.20 mmol), **3b** (730 mg, 1.29 mmol), **4** (1.19 g, 3.88 mmol), eluent: chloroform/THF 5:1 (R_f = 0.09), after elution of symmetrical congener AAAA the mobile phase was changed to chloroform/THF/MeOH 5:1:1 (purified twice). Yield: 198 mg (10%) of green solid; MS (MALDI-TOF): *m/z*: 1506.6 $[M]^+$, 1529.6 $[M+Na]^+$, 1545.6 $[M+K]^+$; HRMS (ESI$^+$): *m/z* calcd for $C_{68}H_{94}MgN_{18}O_8S_6$ $[M+H]^+$: 1507.5755; found: 1507.5775 $[M+H]^+$.

Compound 1cMg: Mg (674 mg, 27.73 mmol), **3c** (620 mg, 0.99 mmol), **4** (911 mg, 2.97 mmol), eluent: chloroform/THF/MeOH 10:2:1 (R_f = 0.14) and then chloroform/THF 10:2 mobile phase was changed after removal of symmetrical congener AAAA to chloroform/THF/MeOH 5:1:1 (purified once). Yield: 130 mg (8%) of green solid; MS (MALDI-TOF): *m/z*: 1594.5 $[M+H]^+$, 1617.5 $[M+Na]^+$; HRMS (ESI$^+$): *m/z* calcd for $C_{72}H_{102}MgN_{18}O_{10}S_6$ $[M+H]^+$: 1595.6279; found: 1595.6282.

General procedure for the synthesis of 1a–cH

Compound **1aMg**, **1bMg** or **1cMg** was dissolved in THF, then TsOH was added and the solution was stirred for 1 h at RT protected from light by an aluminium cover. The solution was concentrated under reduced pressure and diluted with water. The precipitate was collected by filtration and washed with water several times. The crude product was purified by column chromatography on silica gel; the mobile phases are mentioned for each compound below. The purified product was washed with hexane and thoroughly dried under reduced pressure.

Compound 1aH: Compound **1aMg** (275 mg, 0.19 mmol), TsOH (368 mg, 1.93 mmol), eluent: chloroform/THF 5:1 (R_f = 0.30). Yield: 58 mg (21%) of dark green solid; ^{1}H NMR (300 MHz, $CDCl_3$/[D$_5$]pyridine, 25 °C): δ = −1.48 (s, 2H; central NH), 2.25 (s, 18H; C-CH$_3$), 2.27 (s, 36H; C-CH$_3$), 3.72–3.90 (m, 16H; crown-H), 4.28–4.38 (m, 8H; crown-H), 4.38–4.49 ppm (m, 8H; crown-H); ^{13}C NMR (75 MHz, $CDCl_3$/[D$_5$]pyridine, 25 °C): δ = 30.5, 30.6, 30.8, 50.5, 51.21, 51.24, 51.8, 70.0, 70.3, 71.5, 138.6, 139.6, 145.0, 145.3, 150.9, 157.8, 158.8, 160.3 ppm; IR (ATR): $\tilde{\nu}$ = 3307 (central NH), 2953, 2898, 2576, 1519, 1461, 1416, 1362, 1318, 1278, 1246, 1136, 1076, 1028, 969 cm^{-1}; UV/Vis (CH_3CN): λ_{max} (ε) = 670 (64000), 649 (71400), 580 (36600), 469 (26800), 424 sh, 383 (84200 mol^{-1} L cm^{-1}); UV/Vis (THF): λ_{max} (ε) = 671 (71900), 651 (77100), 577 (35200), 469 (29800), 430 sh, 367 (88600 mol^{-1} L cm^{-1}); MS (MALDI-TOF): *m/z*: 1396.5 $[M]^+$; HRMS (ESI$^+$): *m/z* calcd for $C_{64}H_{88}N_{18}O_6S_6$ $[M+H]^+$: 1397.5537; found: 1397.5557.

Compound 1bH: Compound **1bMg** (150 mg, 0.10 mmol), TsOH (132 mg, 0.69 mmol), eluent: chloroform/THF/MeOH 30:4:1 (R_f = 0.52). Yield: 99 mg (67%) of dark green solid; ^{1}H NMR (300 MHz, $CDCl_3$/[D$_5$]pyridine, 25 °C): δ = −1.50 (s, 2H; central NH), 2.23 (s, 36H; C-CH$_3$), 2.24 (s, 18H; C-CH$_3$), 3.71 (s, 8H; crown-H), 3.73–3.85 (m, 16H; crown-H), 4.21 (t, J = 5 Hz, 8H; crown-H), 4.41 ppm (t, J = 5 Hz, 8H; crown-H); ^{13}C NMR (75 MHz, $CDCl_3$/[D$_5$]pyridine, 25 °C): δ = 30.6, 30.8, 31.0, 50.8, 51.32, 51.34, 51.9, 70.2, 70.4, 70.6, 71.2, 138.9, 139.7, 145.2, 145.6, 150.9, 157.8, 159.1, 160.4 ppm; IR (ATR): $\tilde{\nu}$ = 3306 (central NH), 2864, 2583, 1967, 1868, 1830, 1844, 1792, 1772, 1749, 1734, 1717, 1698, 1684, 1670, 1653, 1647, 1636, 1617, 1558, 1541, 1521, 1507, 1497, 1489, 1473, 1458, 1438, 1419, 1362, 1318, 1285, 1233, 1139, 1025, 970 cm^{-1}; UV/Vis (CH_3CN): λ_{max} (ε) = 671 (84200), 650 (95000), 578 (49700), 467 (35200), 427 sh, 365 (113900 mol^{-1} m^3 cm^{-1}); UV/Vis (THF): λ_{max} (ε) = 672 (93000), 652 (102200), 578 (49500), 467 (37800), 424 sh, 366 (119700 mol^{-1} L cm^{-1}); MS (MALDI-TOF): *m/z*: 1484.6 $[M]^+$, 1507.6 $[M+Na]^+$, 1523.6 $[M+K]^+$; HRMS (ESI$^+$): *m/z* calcd for $C_{68}H_{96}N_{18}O_8S_6$ $[M+H]^+$: 1485.6061; found: 1485.6062.

Compound 1cH: Compound **1cMg** (130 mg, 0.08 mmol), TsOH (152 mg, 0.80 mmol), eluent: chloroform/THF/MeOH (R_f = 0.20). Yield: 29 mg (23%) of dark green solid; ^{1}H NMR (300 MHz, $CDCl_3$/[D$_5$]pyridine, 25 °C): δ = −1.49 (s, 2H; central NH), 2.22 (s, 18H; C-CH$_3$), 2.23 (s, 18H; C-CH$_3$), 2.24 (s, 18H; C-CH$_3$), 3.70–3.82 (m, 32H; crown-H), 4.13 (t, J = 5 Hz, 8H; crown-H), 4.50 ppm (t, J = 5 Hz, 8H; crown-H); ^{13}C NMR (75 MHz, $CDCl_3$/[D$_5$]pyridine, 25 °C): δ = 30.6, 30.8, 31.0, 49.8, 51.3, 52.0, 70.2, 70.6, 70.9, 71.0, 71.2, 138.8, 139.6, 145.3, 145.7, 150.9, 157.8, 159.1, 160.5 ppm; IR (ATR): $\tilde{\nu}$ = 3301 (central NH), 2865, 2578, 1954, 1638, 1521, 1467, 1423, 1362, 1318, 1280, 1248, 1137, 1077, 1027, 970 cm^{-1}; UV/Vis (CH_3CN): λ_{max} (ε) = 670 (74600), 650 (85200), 580 (47200), 467 (32000), 424 sh, 365 (102400 mol^{-1} L cm^{-1}); UV/Vis (THF): λ_{max} (ε) = 670 (92400), 652 (102600), 559 (54300), 466 (39500), 428 sh, 367

(120300 $mol^{-1} m^3 cm^{-1}$); MS (MALDI-TOF): *m/z*: 1572.6 $[M]^+$, 1595.5 $[M+Na]^+$, 1611.5 $[M+K]^+$; HRMS (ESI^+): *m/z* calcd for $C_{72}H_{104}N_{18}O_{10}S_6$ $[M+H]^+$: 1573.6585; found: 1573.6600.

General procedure for the synthesis of 1 a–cZn

Metal-free **1 aH**, **1 bH** or **1 cH** was dissolved in pyridine, then anhydrous zinc acetate was added, and the mixture was heated under reflux for 1 h. The mixture was cooled and concentrated under reduced pressure. Water was added and the precipitate was collected by filtration and washed with water several times. The crude product was purified by column chromatography on silica gel. The mobile phases are mentioned for each compound below. The purified product was washed with hexane and dried under reduced pressure.

Compound 1 aZn: Compound **1 aH** (40 mg, 0.029 mmol), $Zn(CH_3COO)_2$ (16 mg, 0.087 mmol), eluent: chloroform/THF 4:1 (R_f = 0.35). Yield: 33 mg (79%) of green solid; ^1H NMR (300 MHz, $CDCl_3$/[D_5]pyridine, 25 °C): δ = 2.27 (s, 54H; C-CH_3), 4.14–4.53 ppm (m, 32H; crown-H); ^{13}C NMR (75 MHz, $CDCl_3$/[D_5]pyridine, 25 °C): δ = 23.97, 24.02, 24.1, 29.69, 29.72, 30.9, 31.1, 50.34, 50.40, 51.41, 51.43, 67.5, 67.8, 70.2, 70.7, 71.8, 106.6, 107.8, 110.4, 142.5, 144.3, 144.5, 144.8, 151.6, 152.9, 157.9, 158.2, 158.7 ppm; IR (ATR): $\tilde{\nu}$ = 2948, 2885, 2864, 1736, 1518, 1458, 1417, 1362, 1295, 1248, 1143, 1096, 975 cm^{-1}; UV/Vis (CH_3CN): λ_{max} (ε) = 654 (153500), 595 (31000), 379 (123800 $mol^{-1} L cm^{-1}$); UV/Vis (THF): λ_{max} (ε) = 654 (152500), 595 (32600), 376 (121500 $mol^{-1} L cm^{-1}$); MS (MALDI-TOF): *m/z*: 1458.4 $[M]^+$, 1481.4 $[M+Na]^+$; HRMS (ESI^+): *m/z* calcd for $C_{64}H_{86}N_{18}O_6S_6Zn$ $[M+H]^+$: 1459.4672; found: 1459.4662.

Compound 1 bZn: Compound **1 bH** (73 mg, 0.049 mmol), $Zn(CH_3COO)_2$ (63 mg, 0.34 mmol), eluent: chloroform/THF/MeOH 50:10:1 (R_f = 0.49). Yield: 43 mg (56%) of green solid; ^1H NMR (500 MHz, $CDCl_3$/[D_5]pyridine, 25 °C): δ = 2.28 (s, 54H; C-CH_3), 3.77 (s, 8H; crown-H), 3.82 (s, 16H; crown-H), 4.20 (t, *J* = 6 Hz, 8H; crown-H), 4.40 ppm (t, *J* = 6 Hz, 8H; crown-H); ^{13}C NMR (125 MHz, $CDCl_3$/[D_5]pyridine, 25 °C): δ = 30.92, 30.95, 31.1, 50.5, 51.41, 51.44, 51.47, 70.4, 70.7, 71.2, 123.9, 136.1, 142.6, 144.4, 144.5, 144.9, 150.0, 150.2, 150.5, 150.6, 151.6, 153.0, 157.9, 158.2, 158.9 ppm; IR (ATR): $\tilde{\nu}$ = 2945, 2895, 1703, 1638, 1519, 1489, 1458, 1421, 1362, 1296, 1233, 1144, 1049, 976 cm^{-1}; UV/Vis (CH_3CN): λ_{max} (ε) = 655 (162400), 596 (34800), 376 (130100 $mol^{-1} L cm^{-1}$); UV/Vis (THF): λ_{max} (ε) = 654 (157900), 594 (34900), 375 (131200 $mol^{-1} L cm^{-1}$); MS (MALDI-TOF): *m/z*: 1546.5 $[M]^+$, 1569.5 $[M+Na]^+$; HRMS (ESI^+): *m/z* calcd for $C_{68}H_{94}N_{18}O_8S_6Zn$ $[M+H]^+$: 1547.5196; found: 1547.5190.

Compound 1 cZn: Compound **1 cH** (25 mg, 0.017 mmol), $Zn(CH_3COO)_2$ (20 mg, 0.11 mmol); eluent: chloroform/THF/MeOH (R_f = 0.34). Yield: 16 mg (62%) of green solid; ^1H NMR (300 MHz, $CDCl_3$/[D_5]pyridine, 25 °C): δ = 2.24 (s, 54H; C-CH_3), 3.74–3.82 (m, 32H; crown-H), 4.08 (t, *J* = 8 Hz, 8H; crown-H), 4.45 ppm (t, *J* = 8 Hz, 8H; crown-H); ^{13}C NMR (75 MHz, $CDCl_3$/[D_5]pyridine, 25 °C): δ = 29.8, 30.8, 31.0, 49.5, 51.33, 51.36, 70.4, 70.6, 70.85, 70.99, 71.08, 142.5, 144.3, 144.4, 144.8, 151.5, 153.0, 157.8, 158.1, 158.8 ppm; IR (ATR): $\tilde{\nu}$ = 2975, 2920, 2850, 1739, 1563, 1515, 1455, 1416, 1362, 1297, 1255, 1233, 1140, 1099, 1043, 976 cm^{-1}; UV/Vis (CH_3CN): λ_{max} (ε) = 656 (137700), 597 (27300), 379 (98260 $mol^{-1} L cm^{-1}$); UV/Vis (THF): λ_{max} (ε) = 655 (134700), 595 (28600), 377 (105200 $mol^{-1} L cm^{-1}$) ; MS (MALDI-TOF): *m/z*: 1634.5 $[M]^+$, 1657.5 $[M+Na]^+$; HRMS (ESI^+): *m/z* calcd for $C_{72}H_{102}N_{18}O_{10}S_6Zn$ $[M+H]^+$: 1635.5720; found: 1635.5712.

Incorporation of 1 bZn into silica nanoparticles (1 bZn@NP)

An emulsion was prepared by dissolving Tween 80 (180 mg) and 1-butanol (0.4 mL) in deionised water (10 mL) under vigorous magnetic stirring and by adding a solution of **1 bZn** (1 mM, 100 μL) in chloroform to the resulting micellar solution. After 1 h, neat silicate precursor triethoxyvinylsilane (10 μL) was added to the emulsion, and the resulting mixture was magnetically stirred for approximately 20 h at RT to ensure completion of sol–gel condensation. Residual chloroform, 1-butanol, and Tween 80 were removed by dialysing the nanoparticle dispersion against deionised water in a 12–14 kDa cutoff cellulose membrane (Spectrum Laboratories, Inc.) for 96 h. For the characterisation of **1 bZn@NP**, see the Supporting Information.

Acknowledgements

The work was financially supported by the Czech Science Foundation (14-02165P) and by Charles University in Prague (SVV 260 183). We wish to thank Jiří Kuneš for NMR spectroscopy measurements, Juraj Lenčo for MALDI-TOF measurements and Lucie Nováková for HRMS data.

Keywords: cations · crown compounds · fluorescent probes · phthalocyanines · sensors

[1] C. J. Pedersen, *J. Am. Chem. Soc.* **1967**, *89*, 7017 – 7036.
[2] X. X. Kong, F. Y. Su, L. Q. Zhang, J. Yaron, F. Lee, Z. W. Shi, Y. Q. Tian, D. R. Meldrum, *Angew. Chem. Int. Ed.* **2015**, *54*, 12053 – 12057; *Angew. Chem.* **2015**, *127*, 12221 – 12225.
[3] T. Schwarze, J. Riemer, S. Eidner, H. J. Holdt, *Chem. Eur. J.* **2015**, *21*, 11306 – 11310.
[4] S. Ast, T. Schwarze, H. Muller, A. Sukhanov, S. Michaelis, J. Wegener, O. S. Wolfbeis, T. Korzdorfer, A. Durkop, H. J. Holdt, *Chem. Eur. J.* **2013**, *19*, 14911 – 14917.
[5] S. Shinkai, T. Ogawa, Y. Kusano, O. Manabe, K. Kikukawa, T. Goto, T. Matsuda, *J. Am. Chem. Soc.* **1982**, *104*, 1960 – 1967; b) M. Natali, S. Giordani, *Chem. Soc. Rev.* **2012**, *41*, 4010 – 4029.
[6] S. Fery-Forgues, F. Al-Ali, *J. Photochem. Photobiol. C* **2004**, *5*, 139 – 153.
[7] P. Holý, J. Koudelka, M. Belohradsky, I. Stibor, J. Zavada, *Collect. Czech. Chem. Commun.* **1991**, *56*, 1482 – 1488.
[8] O. Sato, N. Matsuda, J. Tsunetsugu, *Heterocycles* **2001**, *54*, 439 – 444; b) S. K. Kim, M. Y. Bang, S. H. Lee, K. Nakamura, S. W. Cho, J. Yoon, *J. Inclusion Phenom. Macrocyclic Chem.* **2002**, *43*, 71 – 75.
[9] B. Valeur, I. Leray, *Coord. Chem. Rev.* **2000**, *205*, 3 – 40.
[10] B. Daly, J. Ling, A. P. de Silva, *Chem. Soc. Rev.* **2015**, *44*, 4203 – 4211.
[11] J. R. Lakowicz, *Principles of Fluorescence Spectroscopy*, 3rd ed., Springer, New York, **2006**.
[12] V. Novakova, M. Miletin, K. Kopecky, P. Zimcik, *Chem. Eur. J.* **2011**, *17*, 14273 – 14282.
[13] V. Novakova, M. Lásková, H. Vavřičková, P. Zimcik, *Chem. Eur. J.* **2015**, *21*, 14382 – 14392 .
[14] V. Novakova, L. Lochman, I. Zajícová, K. Kopecky, M. Miletin, K. Lang, K. Kirakci, P. Zimcik, *Chem. Eur. J.* **2013**, *19*, 5025 – 5028.
[15] L. Lochman, J. Svec, J. Roh, V. Novakova, *Dyes Pigm.* **2015**, *121*, 178 – 187.
[16] V. Novakova, P. Reimerova, J. Svec, D. Suchan, M. Miletin, H. M. Rhoda, V. N. Nemykin, P. Zimcik, *Dalton Trans.* **2015**, *44*, 13220 – 13233.
[17] A. Y. Freidzon, A. A. Bagatur'Yants, S. P. Gromov, M. V. Alfimov, *Int. J. Quantum Chem.* **2004**, *100*, 617 – 625.
[18] V. A. Shubert, C. W. Müller, T. S. Zwier, *J. Phys. Chem. A* **2009**, *113*, 8067 – 8079.
[19] P. Zimcik, M. Miletin, V. Novakova, K. Kopecky, M. Nejedla, V. Stara, K. Sedlackova, *Aust. J. Chem.* **2009**, *62*, 425 – 433.
[20] K. Kopecky, D. Šatinský, V. Novakova, M. Miletin, A. Svoboda, P. Zimcik, *Dyes Pigm.* **2011**, *91*, 112 – 119.

[21] V. Novakova, P. Zimcik, M. Miletin, L. Vachova, K. Kopecky, K. Lang, P. Chábera, T. Polívka, *Phys. Chem. Chem. Phys.* **2010**, *12*, 2555 – 2563.
[22] V. Novakova, K. Kopecky, M. Miletin, J. Ivincova, P. Zimcik, *J. Porphyrins Phthalocyanines* **2011**, *15*, 1062 – 1069.
[23] V. Novakova, P. Hladik, T. Filandrova, I. Zajicova, V. Krepsova, M. Miletin, J. Lenco, P. Zimcik, *Phys. Chem. Chem. Phys.* **2014**, *16*, 5440 – 5446; b) A. Cidlina, V. Novakova, M. Miletin, P. Zimcik, *Dalton Trans.* **2015**, *44*, 6961 – 6971.
[24] M. Quintiliani, A. Kahnt, T. Wolfle, W. Hieringer, P. Vázquez, A. Gorling, D. M. Guldi, T. Torres, *Chem. Eur. J.* **2008**, *14*, 3765 – 3775; b) L. Fajari, P. Fors, K. Lang, S. Nonell, F. R. Trull, *J. Photochem. Photobiol. A* **1996**, *93*, 119 – 128.
[25] L. Vachova, V. Novakova, K. Kopecky, M. Miletina, P. Zimcik, *Dalton Trans.* **2012**, *41*, 11651 – 11656.
[26] J. W. Steed, *Coord. Chem. Rev.* **2001**, *215*, 171 – 221.
[27] V. Gutmann, E. Wychera, *Inorg. Nucl. Chem. Lett.* **1966**, *2*, 257 – 260.
[28] C. Reichardt, *Solvents and Solvent Effect in Organic Chemistry*, 3rd ed., Wiley-VCH, Weinheim, **2003**.
[29] G. H. Rounaghi, F. Mofazzeli, *J. Inclusion Phenom. Macrocyclic Chem.* **2005**, *51*, 205 – 210.

Received: October 23, 2015
Published online on January 8, 2016

